THE ASTROPHYSICAL JOURNAL, 466:224–233, 1996 July 20

AN EMPIRICAL TECHNIQUE FOR ASSESSING THE INSTRUMENTAL ERRORS OF 21 CENTIMETER EMISSION LINE ZEEMAN SPLITTING MEASUREMENTS

CARL HEILES
Astronomy Department, University of California at Berkeley, Berkeley, CA 94720; cheiles@astro.berkeley.edu
Received 1995 May 19; accepted 1996 January 24

ABSTRACT

We illustrate a technique for empirically assessing the instrumental errors in 21 cm emission line Zeeman splitting measurements. For altitude-azimuth mounted telescopes this technique can be applied to many positions, but for equatorial telescopes it can be applied only at the celestial poles. Here we apply the technique with the equatorially mounted Hat Creek 85 foot (26 m) telescope by measuring the apparent circular polarization of the 21 cm line in emission toward the north celestial pole (NCP) and its variation with "right ascension" as the polarized beam pattern rotated with respect to the sky. The first and second Fourier components of this variation are equal to the instrumental errors contributed by beam squint and linear polarization, respectively. For the Hat Creek telescope at the NCP, we show that the dominant instrumental error is beam squint. We compare the empirical determination of the beam squint error with the value calculated from the measured beam squint. At the NCP, the instrumental error is fairly small compared to the actual field strength. The NCP has a somewhat larger velocity gradient than is typical, and the beam squint of the Hat Creek Radio Observatory telescope at the NCP was unusually large; we conclude that most measurements of Zeeman splitting in emission made with this telescope are reliable.

Subject headings: atomic processes — ISM: magnetic fields — polarization — radio lines: ISM

1. INTRODUCTION

The interstellar magnetic field in H I regions can be measured from the Zeeman splitting of the 21 cm line as seen in both absorption and emission. Emission measurements have the great advantage that one can look anywhere, so that the field in interesting regions can be measured and mapped. However, emission measurements are prone to instrumental errors. As reviewed by Troland & Heiles (1982, hereafter TH), Zeeman splitting is measured from the circular polarization (Stokes V component)[1] of the 21 cm line profile. Zeeman splitting is the difference in line frequency Δv between the two polarizations. The 21 cm line is always much wider than this difference, which causes the V spectrum to look like the frequency derivative of the total intensity I profile with amplitude proportional to the frequency difference Δv. For this case, the line-of-sight component of the field $B_{\|}$ is equal to $0.36\Delta v$ μG, where Δv is in hertz.

Observing Zeeman splitting amounts to observing the sky with a "circularly polarized beam," i.e., the Stokes V beam. In practice, this V beam is not a "clean beam" because it has sidelobes. TH used both their empirical investigations of the 85 foot telescope at the Hat Creek Radio Observatory (HCRO) (below denoted the "HCRO telescope" or the "85 foot telescope") and theoretical investigations published by others to classify these V sidelobes three primary ways:

1. *Beam squint, in which the two circular polarizations point in different directions with a separation and direction* $\boldsymbol{\Psi}_B$.[2]—This produces a "two-lobed" V beam, in which the lobes are located on opposite sides of beam center, have opposite signs with amplitude proportional to Ψ_B, and are separated by about one half-power beamwidth (HPBW). This two-lobed structure responds to the first derivative of the 21 cm line on the sky. If the line has a velocity gradient ∇v, then this structure produces a velocity difference $\Delta v = \nabla v \cdot \boldsymbol{\Psi}_B$ between the two circular polarizations. As discussed in § 3.2 below, the representative value for the instrumental error from beam squint with the HCRO telescope is 0.7 μG.

2. *The presence of residual linear polarization in what should be pure circular polarization.*—In other words, the observations are made with slight elliptical polarization instead of pure circular polarization. This produces a "four-lobed" V beam, in which two lobes on opposite sides of beam center have the same sign and two lobes rotated 90° have the opposite sign. This four-lobed structure responds to the second derivative of the 21 cm line on the sky. As explained by TH, it is easy to measure this astronomically and use the result to adjust the polarimeter for pure circular polarization. In practice with the HCRO telescope, we have found no evidence for any significant contribution from this effect, and this is illustrated by the following: Heiles (1989, § II*a*) unknowingly observed many positions with a poorly adjusted polarimeter and, after discovering the maladjustment and correcting it, reobserved these positions. He found no discernible difference.

3. *Instrumental polarization outside the main beam and at large angles from beam center.*—This includes sidelobe structure at all scales larger than the main telescope beam. The total power in these "distant sidelobes" is nontrivial:

[1] In the present and our previous papers, we follow the definition of Stokes parameters given by Kraus (1966), to wit: (1) We use the IEEE definition, in which left circular polarization (LCP) rotates clockwise as seen by the receiving antenna; and (2) V = LCP − RCP.

[2] In this paper, vector quantities on the sky are indicated by boldface letters, and the same letters in lightface type represent the magnitudes of the vectors.

they are weak, but they cover a very large solid angle; furthermore, they tend to be highly elliptically polarized. These "distant sidelobes" are a result of telescope surface roughness and the feed leg structure. TH found that within 4° of beam center the polarized sidelobe structure is "jumbled and irregular." They did not explicitly state the fact that this structure is so weak that its existence is barely measureable. To see it, TH tried using Cas A, the strongest continuum "point source" available; Cas A was too weak to reliably map this structure. TH also tried using the Sun to map it, but the Sun is not sufficiently close to being a point source to probe this structure, whose angular scale is comparable to the beam squint. TH were successful in using the Sun to probe the feed leg rings, which have a much larger angular scale (see their Fig. 1). TH found that these sidelobes, even with their larger total power, are unimportant in practice because they produce broad, weak features in the V spectrum that are easy to distinguish from the narrower features produced by H I clouds.

This threefold classification is equivalent to a two-dimensional Taylor expansion of the polarized sidelobe structure. TH found this to be an excellent description of the actual polarized sidelobes for the HCRO telescope. This is reflected in the fact that TH made complete maps of the sidelobes only near the beginning of their efforts, in the late 1970s; it rapidly became clear that it was much easier and more efficient to parameterize the maps with the above classification. In fact, no complete maps of the V beam remain available for the HCRO telescope.

The appropriateness of this threefold classification also applies to the Green Bank 140 foot (43 m) telescope, as can be seen in the maps of its V beam presented by Verschuur (1969, 1989). Verschuur's (1969) Figure 2 presents the V beam pattern for the 140 foot telescope as it was in the late 1960s. At that time, it was very well described by beam squint with a peak-to-peak amplitude of about 1.4%; this corresponds to a beam squint $\Psi_B \approx 7'$. Our maps of the complete polarized sidelobe structure of the HCRO telescope always produced similar results, although with much smaller beam squint (§ 3.1 below). Verschuur's (1989) Figure 1 presents the 140 foot polarized beam structure as it was in the late 1980s, and shows a drastic difference: the newer map shows primarily the four-lobed pattern of our category (2) with a little beam squint. The 1960s version of the beam pattern made the 140 foot telescope unsuitable for Zeeman-splitting measurements of H I in emission because the beam squint contribution to instrumental error would have been excessive. However, the 1980s version, with its small beam squint but higher second derivative component, was satisfactory—as shown by the fact that Verschuur reobserved four positions that had previously been observed with the HCRO telescope and found excellent agreement in three, as discussed in some detail by Heiles (1991).

More recently, Verschuur (1993) has claimed that "claims of Zeeman effect detection in H I emission features . . . . based on observations made with presently available single-dish radio telescopes cannot be regarded as reliable." At the time of his paper, the HCRO telescope had already been destroyed, but he meant his claim to apply to that telescope as well as to other telescopes that still exist. We believe his claim to be incorrect. His claim is based on his estimates of the instrumental effects of near-in sidelobes of the V beam, which in turn are based on new measurements (Verschuur 1995a, b) of the 140 foot telescope's V beam and of the apparent circular polarization of the 21 cm line in emission at many positions. His new estimates disagree with older ones made by both himself and others. We have explained the reasons for these disagreements elsewhere (Heiles 1996).

The present paper presents a general technique for empirically assessing the instrumental errors of emission-line Zeeman splitting measurements, the specific application of which to the HCRO telescope having the additional benefit of showing that its results are generally reliable. This paper addresses the interaction of beam squint with H I velocity gradients, and before proceeding further we first address three related details:

1. We explicitly define the term "velocity gradient." In accordance with the standard definition of vector differential calculus (e.g., Kaplan 1952), the magnitude of the gradient is

$$\nabla v = [(\delta v/\cos b\ \delta l)^2 + (\delta v/\delta b)^2]^{1/2}\ ;$$

here we have written the definition in terms of Galactic coordinates as an example. We evaluate the derivatives numerically from the differences between closely spaced profiles. Consider one pair of profiles: we construct a difference and average profile. From these difference and average profiles, we calculate the velocity difference employing exactly the same least-squares fitting technique that we use to derive the magnetic field strength from a V and an $I/2$ profile (eq. [1] of TH). The derivative is equal to the velocity difference divided by the true (great-circle) angular separation.

2. The total velocity gradiant is what contributes to the instrumental error. There are two components to the gradient. One (the "GAS") involves the motion of gas in some particular reference frame; the second (the "EARTH") involves the Earth's (more precisely, the telescope's) motion with respect to that same reference frame. In the present paper, we choose the local standard of rest (LSR) as the particular reference frame. The EARTH contribution continually changes because the Earth orbits the Sun.

If one directly measures the velocity gradient at the telescope, one might follow the standard procedure and make a five-point map. For these five points one should always use the local oscillator frequency that is appropriate to the central position, *without* using different Doppler corrections for the different positions; this properly measures the total velocity gradient for the particular time of year of the measurement.

Alternatively, one can evaluate the velocity gradient from a catalog of H I profiles. With this procedure, the GAS contribution is accounted for because velocities are always given with respect to the LSR. However, the EARTH contribution is not accounted for, and one should add it vectorially to the GAS contribution; obviously, the result depends on the time of year. It is easy to estimate the maximum contribution of the EARTH component. The maximum combination of the Earth's orbital velocity and the solar velocity with respect to the LSR is about 45 km s^{-1}, and the maximum derivative is about 0.8 km s^{-1} deg^{-1}. This is comparable to the average interstellar gradient (§ 3.2 below).

3. Finally, we consider whether an *intensity* gradient, in the absence of a velocity gradient as defined above, can produce a false instrumentally based result for Zeeman splitting. As discussed by TH, the Zeeman splitting is gener-

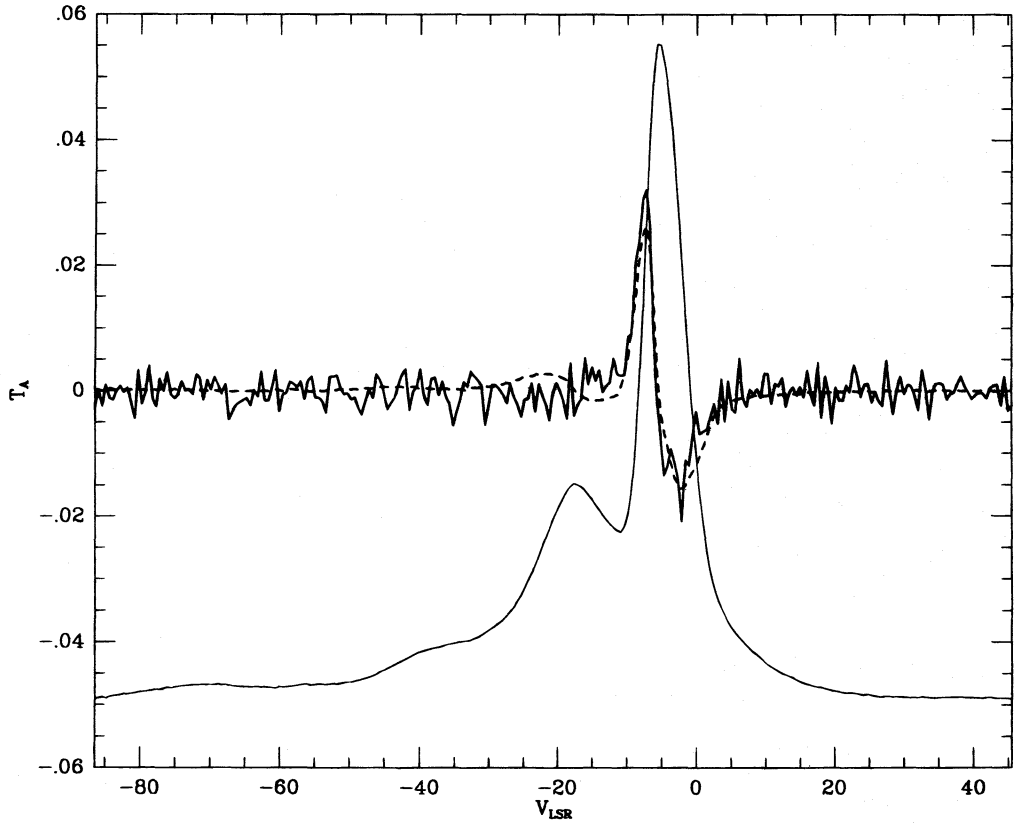

FIG. 1.—Grand average of (half the) total intensity and the circularly polarized (Stokes $I/2$ and V) spectra toward the NCP. The thick solid line is the V spectrum, the thin line the $I/2$ spectrum. On the vertical scale, the units refer to the V spectrum and are antenna temperature in kelvins. . The antenna temperature at the peak of the $I/2$ spectrum is 22.6 K. The dashed line is a least-squares fit of the V spectrum to the frequency derivative of the I spectrum; the resulting line-of-sight magnetic field is $B_{\|} = 8.9 \pm 0.3$ μG. The relation of intensities between the two spectra is exact, but the overall intensity scale is not well calibrated and may be in error by as much as 20%.

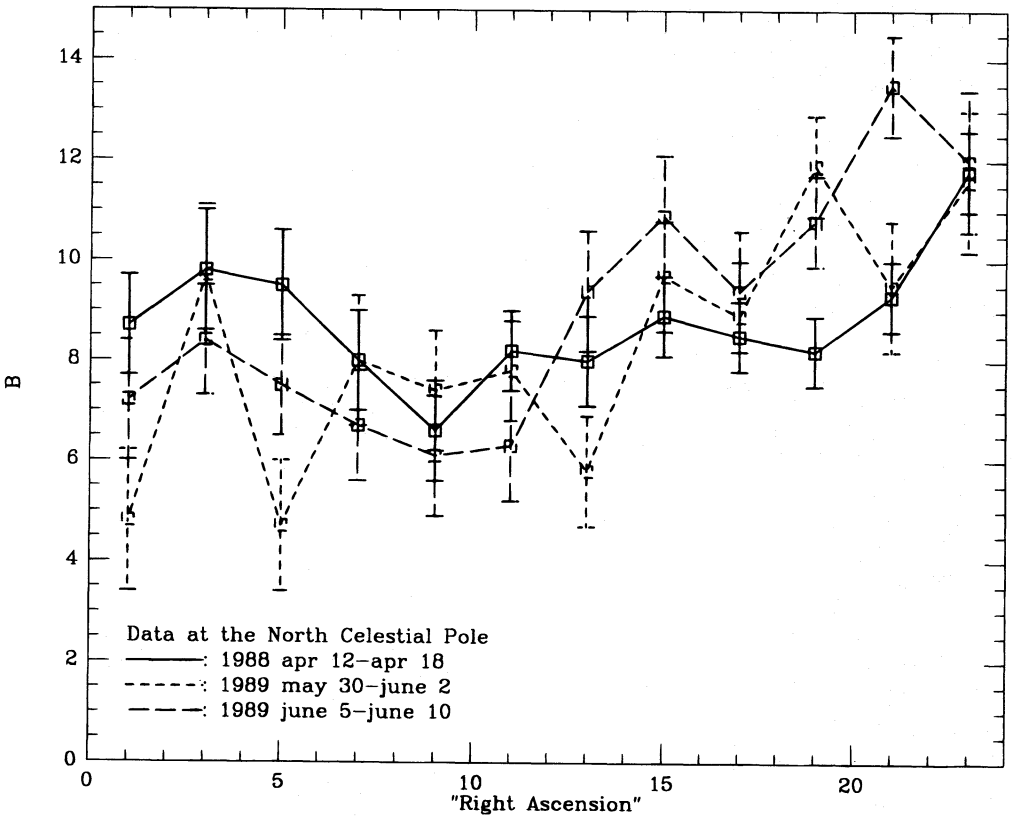

FIG. 2.—Derived $B_{\|}$ (in μG) vs. "right ascension" (in hours) for the three observing sessions

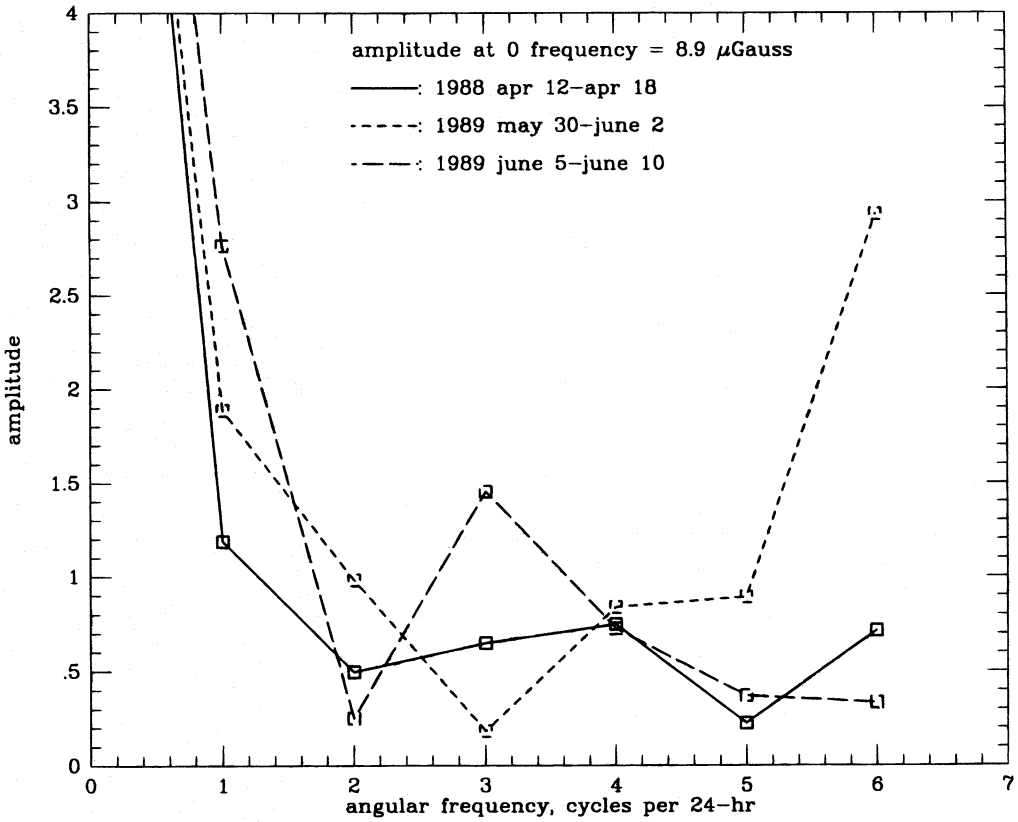

FIG. 3.—Amplitudes (in μG) of the Fourier components of the data in Fig. 2. Instrumental effect 1, beam squint, has 1 cycle per 24 hr; effect 2, linear polarization, has 2 cycles per 24 hr.

ally derived by fitting both a frequency offset and a gain difference between the two profiles of opposite circular polarization. The result is sensitive only to frequency differences. This procedure eliminates the possibility that an intensity gradient can produce a false detection of Zeeman splitting.

In the present paper we describe an *empirical* technique that *directly* evaluates the instrumental contribution of beam squint and linear polarization (error contributions 1 and 2 above). This is in contrast to the usual procedure of using separate, independent measurements of beam squint and of the velocity gradient to *calculate* the instrumental contribution.

This *empirical* technique employs rotation of the beam pattern with respect to the sky. For an altitude-azimuth mounted (alt-az) telescope, this rotation occurs naturally as a position is tracked. However, with an equatorial telescope, the beam pattern remains fixed on the sky during tracking (apart from changes produced by gravitational deflection and the like). Nevertheless, there is one position for which rotation can be made to occur: the celestial pole. The north celestial pole [NCP: $(l, b) \approx (123°, 27°)$] contains a bright H I filament and is part of a region that is well studied in CO and 100 μm emission (e.g., Heithausen & Thaddeus 1990). Heiles (1989) has measured $B_{\|}$ with H I Zeeman splitting in emission for many positions in the filament; typically, $B_{\|} \sim +10\,\mu$G.

In the present paper we apply this technique at the NCP using the HCRO telescope. We also explicitly discuss the beam squint of the Hat Creek telescope and the velocity gradient at the NCP, so that we can compare the direct *empirical* measurement with the *calculation* of the instrumental contribution from beam squint. Finally, we show that for typical positions, contribution 1 above is important at the 0.7 μG level for the HCRO telescope—and is therefore usually unimportant in practice, because published fields are typically several times larger.

2. ILLUSTRATION OF THE TECHNIQUE: EMPIRICAL MEASUREMENT OF THE INSTRUMENTAL ERROR AT THE NCP

We observed the NCP in three independent observing sessions, once in 1988 April and twice in 1989 May–June during two sessions, between which the receiver was reworked and readjusted. We pointed toward the NCP at zero hour angle and turned off the telescope drive for several days, recording data all the while. We then binned the data into 12 2 hr intervals. It is difficult for most equatorially mounted telescopes to point at the NCP, and the HCRO telescope was no exception: we had to remove protective structural members and bypass protective electric circuitry.

We measure the apparent magnetic field strength $B_{\|}$ separately and independently for each of the 12 positions. We then Fourier analyze the 12 results with respect to time ("right ascension" of R.A.). Consider first error 1, with a two-lobed pattern. Suppose that at a particular R.A.$_+$ the pattern is "lined up" with the direction of the local 21 cm line gradient; the subscript + means that at this R.A. the instrumental error is maximum and is positive in sign. Twelve hours later the pattern will have rotated 180° on the

sky, the positive and negative lobes will have interchanged, and the instrumental error will be the same in magnitude but negative in sign. Thus, the instrumental error produced by the two-lobed pattern produces a Fourier component with one cycle per 24 hours (the "first Fourier component") whose amplitude is equal to the instrumental error from this effect. The situation is similar for error 2: Suppose that at R.A.$_+$ it is lined up with the local second derivative. Six hours later it will have rotated 90° on the sky, the positive and negative lobes will have interchanged, and the instrumental error will be the same in magnitude but negative in sign. Thus, the instrumental error produced by the four-lobed pattern produces a Fourier component with two cycles per 24 hours (the "second Fourier component") whose amplitude is equal to the instrumental error from this effect.

Figure 1 shows the average of all data for the three observing sessions. The dashed line has the shape of the derivative of the I spectrum and is a good fit to the V spectrum, with $B_{\|} = 8.9 \pm 0.3$ μG; this is in excellent agreement with the nearby measurements of Heiles (1989).

Figure 2 shows $B_{\|}$ as a function of R.A. for the three observing sessions. There is a systematic variation of $B_{\|}$ with R.A. from $\sim$6 to 12 μG, indicating the contribution of instrumental errors. Figure 3 presents the Fourier amplitudes for the three data sets. On Figure 3, the zero-frequency components are the average fields, which were 8.8 ± 0.4, 8.4 ± 0.6, and 9.1 ± 0.6 μG for the three data sets in order of time; we regard this as satisfactory agreement. The first Fourier component is significantly higher than the others, while the second is comparable to them and is probably not significant. We consider components 2–6 as indicative of the uncertainties, and for each data set our quoted error for the amplitude of component 1 is the average of the amplitudes of components 2–6.

The amplitudes of the first Fourier components constitute empirical measurements at this position for instrumental effect 1 for the three data sets, which are 1.19 ± 0.57, 1.89 ± 1.17, and 2.76 ± 0.63 μG, again in order of time. From the phases of the first Fourier components we can determine the R.A.'s at which the beam squint produced zero effect; these are 5.33, 1.40, and 1.80 hr, respectively (and, or course, also 12.0 hr later). The results appear to be significantly different, which probably reflects variation in the beam squint over time (see last paragraphs of § 3.1).

3. CALCULATION OF THE INSTRUMENTAL ERROR FROM BEAM SQUINT AT THE NCP

The calculation of the instrumental error from beam squint at the NCP requires knowledge of two quantities: the beam squint and the velocity gradient.

3.1. *Beam Squint of the Hat Creek Telescope*

During our many years of Zeeman-splitting observations at HCRO, we measured and occasionally adjusted the system to minimize beam squint, typically obtaining data for a full day or more at the beginning of and periodically during an observing session. Before the summer of 1989, which applies to the present paper, the only records of this measurement and adjustment process were generated on computer-printed paper, and these were generally dicarded soon after the process was finished. During the summer of 1989 we installed a new control computer, and the records were stored on magnetic disk and then transferred to magnetic tape. These tapes are now unavailable, and consequently we are unable to retrieve most of these data files; the data file presented below in Figures 4 and 5 was fortuitously saved on disk and is the only appropriate one that remains available. We will discuss this data set in detail. This data set should be fairly representative of the typical one, but subject to the important caveat stated in the last paragraph of § 3.1.

We note parenthetically that nearly all of the time linear polarization was so small in the HCRO system that it could not be detected by observations of strong continuum sources; the peak-to-peak amplitude of the four-lobed pattern was less than 0.1%. We measured the beam squint using switched circular polarization observations of strong unresolved continuum sources, using the indentical switching apparatus we used for Zeeman-splitting observations. For each source we observed on a nine-point grid centered on the source and least-squares fitted the results to the appropriate derivative of a Gaussian.

Beam squint is produced if the electrical axis of the horn is not parallel to the electrical axis of the paraboloid, i.e., if the horn is not "pointing" exactly at the center of the paraboloid. We note parenthetically that other asymmetries in the location of the feed produce no circular polarization effects to first order (Chu & Turrin 1973). The displacement between the two circularly polarized beams is perpendicular to the offset direction of the feed.

Consider the effect of gravitational deflection on beam squint. For an equatorially mounted telescope at hour angle zero, as a function of declination the gravitational deflection should be in the north-south direction and produce beam squint only in the east-west direction. Conversely, as a function of hour angle the gravitational deflections are primarily (but certainly not wholly) in the east-west direction, and the beam squint should change mainly in the north-south direction. We observed these effects early on with the HCRO telescope.

To eliminate these effects, we equipped the HCRO telescope with a laser and mirror servo system, which measured the mechanical tilt of the feed with respect to the center of symmetry of the telescope's surface and kept the tilt from changing (Heiles 1988, § II). This was largely but not completely effective, probably because the true vertex of the paraboloid moved with respect to the center of symmetry of the telescope surface as the telescope was moved. As our telescope system evolved, we changed the mechanical mounting structure for the feed in an accidentally fortuitous was such that the gravitational deflection of the feed structure compensated (not perfectly, but mostly) for that of the feed legs; after this change, the improvement produced by the laser servo system became marginal and, because of its complexity and imperfect reliability, some time later we discontinued its use. All data in this paper were taken without the laser servo system.

Figures 4*a* and 4*b* show measurements of the north-south beam squint versus hour angle for the period 1991 December 29–30. The scatter of the points indicates the dispersion arising from the signal-to-noise ratio, which depends on the continuum source intensity. We divide the data into two portions, one for sources whose declinations are south of the terrestrial latitude of the telescope (for which gravity pulls south on the feed structure) and one north. The "southern" sources in Figure 4*a* (declination $\lesssim$40°) exhibit more hour-angle dependence than the "northern" ones in

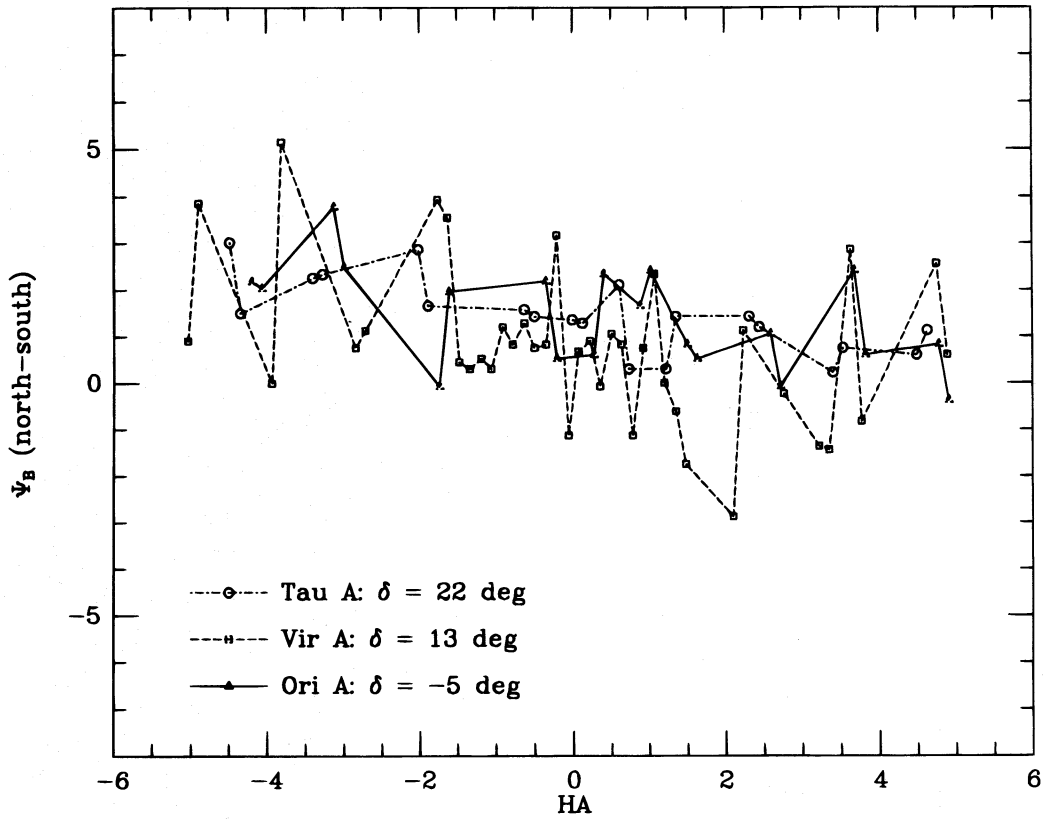

FIG. 4*a*

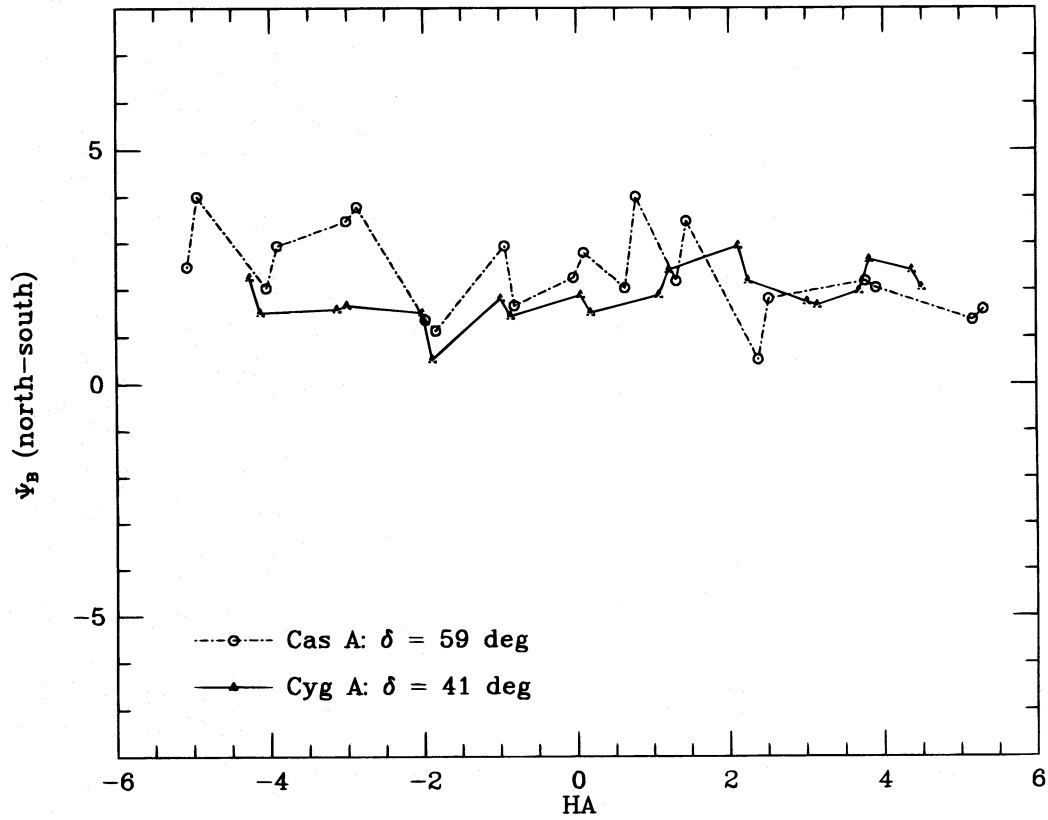

FIG. 4*b*

FIG. 4.—(*a*) North-south beam squint Ψ_B (in arcseconds) vs. hour angle (in hours) for "southern" (declination $\lesssim 40°$) sources. (*b*) North-south beam squint Ψ_B (in arcseconds) vs. hour angle (in hours) for "northern" (declination $\gtrsim 40°$) sources.

Figure 4*b*. In addition, the "northern" sources have somewhat higher beam squint than the "southern" sources. The compensation for gravitational deflection mentioned above should have largely eliminated the positional dependence of beam squint; as mentioned above, we believe that this behavior reveals a large-scale deformation of the telescope surface. Our belief is also based on a sudden jump in pointing correction coefficients near declination 40° and our impression that when the telescope was slewing in declination it would occasionally emit a loud "click" as it crossed declination ~40°.

Figure 5 is similar to Figure 4, except that it shows the east-west beam squint. The east-west squint exhibits very little change with either hour angle or declination.

During the Christmas holidays of 1991, the north-south beam squint is systematically positive, particularly for "northern" sources. This is not as bad as it seems, because during this period we were mapping the magnetic field in the Orion region, near declination −5°. The best adjustment would have had zero beam squint for hour angle zero at declination −5°, so our adjustment was not quite optimum. This nonoptimal condition is unusual because we would routinely adjust the beam squint for the declination range of interest before every observing session and periodically check the adjustment (readjustment was rarely necessary).

The hour-angle variation of beam squint was not eliminated either with the laser servo system or with the new feed mounting structure. Nevertheless, we could observationally eliminate the hour-angle variation by observing a given position over an hour-angle range that was centered near zero so as to average the beam squint over hour angle. Thus, in practice the beam squint was almost never worse than the value at hour angle zero for declination −5° shown in Figure 4*a*. To estimate this, we imagine a smooth line drawn through the points and ignore the departure of individual points from this line, which are simply the random errors resulting from the signal-to-noise ratio. This provides a generously conservative typical value $\Psi_B \lesssim 2'$.

Beam-squint data for 1988 spring and 1989 summer, when we made the observations presented herein, are unavailable. During 1988 summer we began our large 174 position map of the general region near Orion (paper in preparation), and we can only *assume* that the observations herein are characterised by Figures 4 and 5. The beam squint depends on declination, and there are no strong continuum sources above declination 59°, so we must extrapolate Figure 4*b* to declination 90°. This provides our estimate for the beam squint at the NCP, $\Psi_B = 3'$.

We emphasize that this estimate for beam squint is subject to the caveat that our assumption for beam squint is correct, namely, that the beam squint was, in fact, optimized for sources near the declination of Orion. Unfortunately, we have no records of what the adjustment actually was. We will see below that this assumption provides good agreement for the results of the 1989 data set but very poor agreement for the 1988 data set. We can only surmise that the poor agreement for 1988 occurs because then, in 1988 April, the adjustment was optimized for northern sources. We believe that this was, in fact, the case: it is the 1988 April data that were quoted in Heiles (1988), and our recollection is that the adjustment was optimized for northern sources so as to obtain a realistic estimate of actual instrumental errors for our measurements of the NCP shell. Nevertheless, we arrived at this belief only after obtaining the poor agreement, and in the spirit of the scientific method we emphasize our uncertainty regarding this adjustment and, concomitantly, our uncertainty regarding the predicted effects of beam squint in the present paper.

3.2. H I *Velocity Gradients in the Sky and the Typical Instrumental Error from Beam Squint*

Figure 6 shows the statistics of $|\delta v/\cos b\ \delta l|$ derived from the Heiles & Habing (1974) H I survey. These data were derived in the following manner. Data points for the survey were taken at constant latitude and spaced in Galactic longitude by 0.°3/cos b, which is half the telescope beamwidth. The signal-to-noise ratio of adjacent profiles was inadequate to accurately define the velocity gradient. To increase the signal-to-noise, we averaged two adjacent points to produce one profile, and then the next two adjacent points to produce a second; these averages lie 0.°6/cos b apart. We calculated the velocity derivative $|\delta v/\cos b\ \delta l|$ from these two.

If there is no preferred direction for velocity change, then the ensemble average of the total velocity gradient $\langle \nabla v_{\rm GAS} \rangle$ is $2^{1/2} \langle |\delta v/\cos b\ \delta l| \rangle$. From Figure 6 we obtain $\langle |\delta v/\cos b\ \delta l| \rangle = 0.52$ km s^{-1} deg^{-1}, so that $\langle \nabla v_{\rm GAS} \rangle = 0.73$ km s^{-1} deg^{-1}. The median $|\delta v/\cos b\ \delta l|$ is 0.42 km s^{-1} deg^{-1} and is in some ways more appropriate than the mean; however, here we use the mean to obtain a less optimistic estimate for the typical instrumental error. The EARTH velocity gradient must be vectorially added to the GAS gradient; because there is no correlation between the two directions, we combine the approximate EARTH rms value of 0.7 km s^{-1} deg^{-1} (§ 1) in quadrature with $\langle \nabla v_{\rm GAS} \rangle$ to obtain $\langle \nabla v \rangle = 1.0$ km s^{-1} deg^{-1} for the representative total velocity gradient. The beam squint interacts with the total velocity gradient, and, because there is no correlation between the two directions, the beam squint will typically see only $\langle \nabla v \rangle / 2^{1/2}$. Thus, we adopt $\nabla v = 0.7$ km s^{-1} deg^{-1} as the typical total velocity gradient seen by the beam squint.

The typical beam squint in practice is $\Psi_B \lesssim 2'$ (§ 3.1 above). With this the typical instrumental error contribution from beam squint is ~0.7 μG. Of course, this is a representative value in the rms sense, and some positions will have larger errors.

3.3. *The* H I *Velocity Gradient at the NCP*

We used the new Dwingeloo H I survey (Hartmann 1994; Hartmann & Burton 1995) to evaluate the GAS contribution to the velocity gradient at the NCP. Near the beginning of 1989, the NCP had precessed to $(l, b) = (122.°95, 27.°19)$. This lies near one of the Dwingeloo survey's grid points $(l_0, b_0) = (123.°0, 27.°0)$. We evaluated the GAS gradient by using the four nearest grid points oriented along the cardinal directions $\hat{\boldsymbol{l}}$ and $\hat{\boldsymbol{b}}$, using the procedure described in § 1. We did not use the whole H I line profile, because, although the whole profile exhibits velocity structure, only the intense peak exhibits a magnetic field; we used only the velocity range of the peak to calculate the gradient, −11 to +36 km s^{-1}. We obtained $\nabla v_{\rm GAS} = (0.68 \pm 0.08)\hat{\boldsymbol{l}} - (0.22 \pm 0.08)\hat{\boldsymbol{b}}$ km s^{-1} deg^{-1}, where $\hat{\boldsymbol{l}}$ and $\hat{\boldsymbol{b}}$ are unit vectors whose lengths are true great-circular angular distance. [This means that the numerical coefficient of $\hat{\boldsymbol{l}}$ is equal to $\delta v/(\cos b\ \delta l)$.]

We used the HCRO observing software to calculate the LSR Doppler corrections for the above points for dates

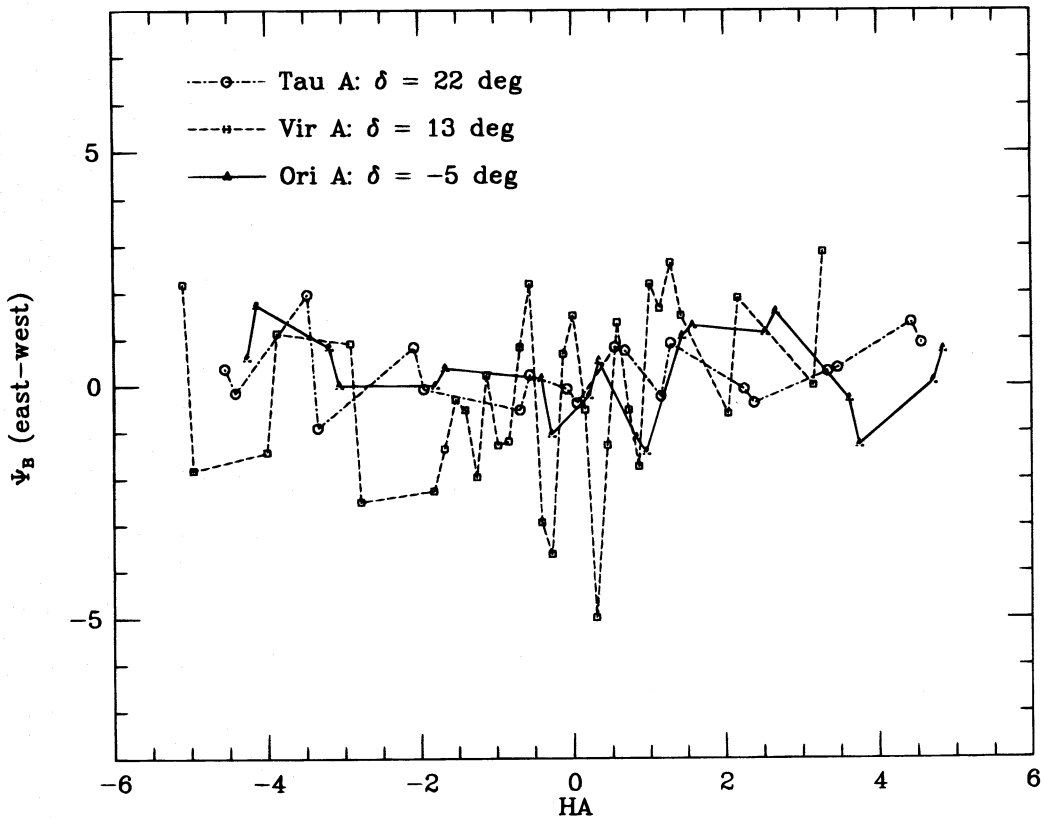

FIG. 5*a*

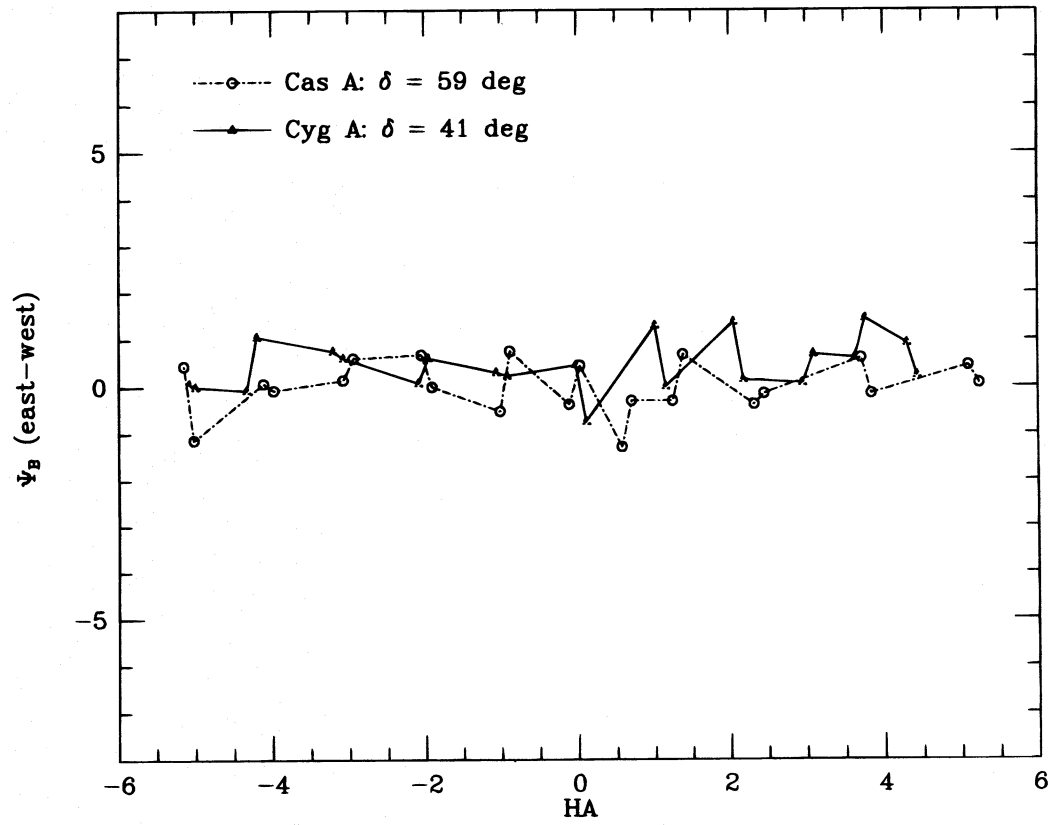

FIG. 5*b*

FIG. 5.—(*a*) East-west beam squint Ψ_B (in arcseconds) vs. hour angle (in hours) for "southern" (declination $\lesssim 40°$) sources. (*b*) East-west beam squint Ψ_B (in arcseconds) vs. hour angle (in hours) for "northern" (declination $\gtrsim 40°$) sources.

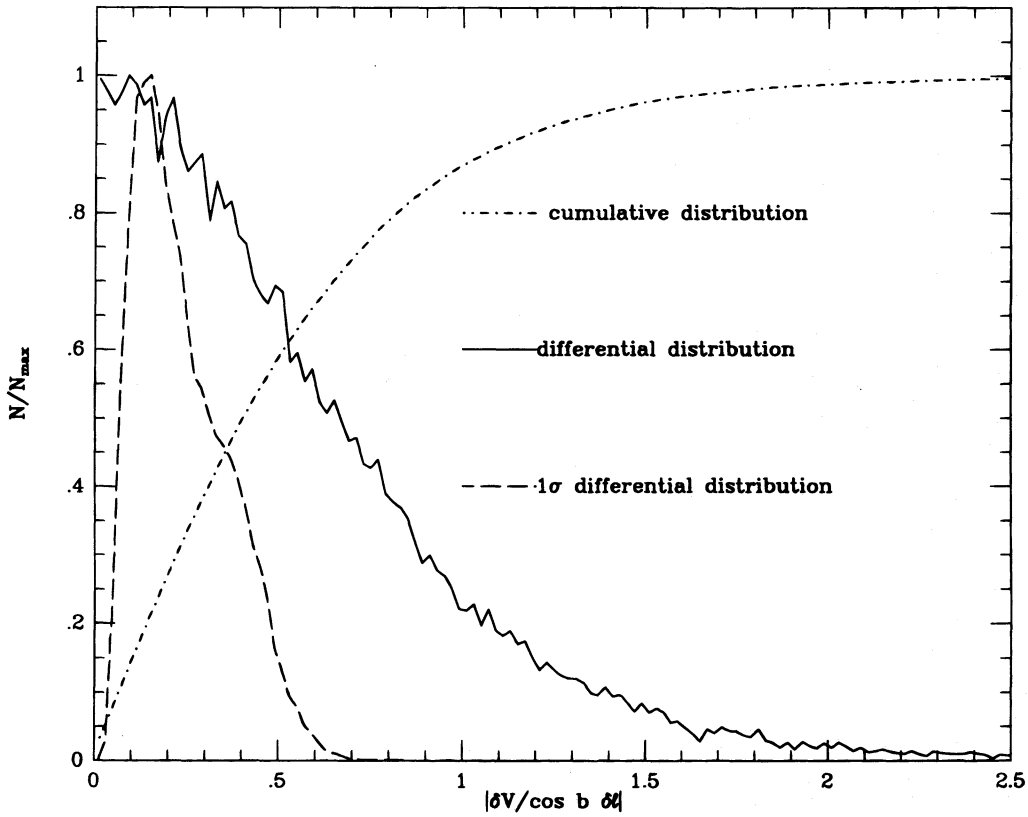

FIG. 6.—Distributions of $|\delta v/\cos b\ \delta l|$ (in km s^{-1} deg^{-1}), derived using the least-squares fitting technique described in § 3.2. The solid line is the differential distribution (*histogram*), and the dash-dot-dash line the cumulative distribution $|\delta v/\cos b\ \delta l|$. The dashed line is the histogram of the 1 σ uncertainty in the derived values of $|\delta v/\cos b\ \delta l|$. The number of points in this sample is $N_{max} = 39{,}332$.

centered near the two observing periods. We obtained $\nabla v_{EARTH} = 0.76\hat{l} + 0.05\hat{b}$ km s^{-1} for the 1988 period and $\nabla v_{EARTH} = 0.56\hat{l} + 0.37\hat{b}$ km s^{-1} deg^{-1} for the 1986 periods.

Adding the GAS and EARTH contributions vectorially gives the magnitude of the velocity gradients, which are $\nabla v = 1.45\hat{l} - 0.17\hat{b}$ and $1.23\hat{l} + 0.15\hat{b}$ km s^{-1} deg^{-1} for the 1988 and 1989 periods, respectively. The corresponding amplitudes are 1.45 and 1.24 km s^{-1} deg^{-1}, and the Galactic position angles[3] of the gradients are P.A.$_{Gal} = +97°$ and $+83°$, respectively.

4. COMPARISON OF THE EMPIRICAL MEASUREMENT AND THE CALCULATION OF THE INSTRUMENTAL ERROR FROM BEAM SQUINT AT THE NCP

First we *calculate* the instrumental error contribution to the measured magnetic field from beam squint at the NCP. In § 3.3 we found the velocity gradients at the NCP to be 1.45 and 1.24 km s^{-1} deg^{-1} for the 1988 and 1989 observing periods. In § 3.1 we estimated the beam squint at the NCP to be 3″ under the assumption discussed in the last two paragraphs of § 3.1. The calculated instrumental error from beam squint is the product of the gradient and beam squint, converted to frequency and then to equivalent magnetic field. This provides 2.04 and 1.73 μG for the 1988 and 1989 observing periods, respectively.

We now calculate the expected R.A. for which the beam squint contribution is zero. The assumed beam squint is oriented north-south (§ 3.1), which means that the position angle of the zero line of the beam squint is P.A.$_{Gal,\,B=0} = 15(6.82 - \text{R.A.})$, where P.A. is in degrees and R.A. in hours. The beam squint should produce zero response when its zero line has the same position angle as the velocity gradient. This occurs at R.A. = $0^h.38$ and $1^h.28$, respectively, for the two observing periods.

In § 2 we *empirically* determined the beam squint contributions. For the two 1989 periods the predicted amplitude is 1.73 μG, while the observed amplitudes are 1.89 ± 1.17 and 2.76 ± 0.63 μG, or 1.1 and 1.6 times the predicted amplitudes. The predicted R.A. for zero effect is $1^h.28$, and the observed R.A.'s are $1^h.40$ and $1^h.80$, differences of 1° and 8°. We regard these as good agreement.

For the 1988 period the predicted amplitude is 2.04 μG, while the observed amplitude is 1.19 ± 0.57 μG, or 0.6 times the predicted amplitude. The predicted R.A. for zero effect is $0^h.35$, and the observed R.A. is $5^h.33$, a difference of 75°. We regard this as unacceptably poor agreement because the phase discrepancy is uncomfortably close to the maximum possible discrepancy of 90°. We suspect, but have no way to verify, that the disagreement for the 1988 data reflects a different beam squint adjustment, as discussed in the concluding paragraphs of § 3.1.

5. SUMMARY AND CONCLUDING REMARKS

In this paper we illustrate a general technique for empirically measuring the instrumental errors of Zeeman splitting of the 21 cm line in emission. In § 2 we used the HCRO 85 foot telescope to measure the time variation of the V spectrum toward the NCP as the polarized sidelobes rotated

[3] The position angle with respect to Galactic coordinates, P.A.$_{Gal}$, is defined as zero when pointing toward $b = 90°$ and increasing toward increasing l.

with respect to the sky. The first and second Fourier components of the variation are equal to the instrumental errors contributed by beam squint and linear polarization. In § 3 we calculated the instrumental beam squint contribution from the measured beam squint and velocity gradient. We compared the measurements and calculations in § 4 and found good agreement for the 1989 data for both amplitude and direction. We suspect, but have no way to verify, that the unacceptable agreement for the 1988 data reflects a different beam squint adjustment, as discussed in the final paragraphs of § 3.1.

In § 3.2 we derived the statistical distribution of the H I line gradient of the northern high-latitude sky, including only the GAS contribution, and then included the EARTH contribution in a statistical sense. The rms total velocity gradient is about 1.0 km s^{-1} deg^{-1}. The NCP has a somewhat larger velocity gradient, about 1.4 km s^{-1} deg^{-1}. In § 3.1 we found the typical beam squint of the HCRO telescope to be $\Psi_B \lesssim 2'$ and the probable value at the NCP to be 3′. These lead to typical beam squint instrumental effects of 1.4 and 0.7 μG for other regions near the NCP (as in Heiles 1988) and for generally typical regions, respectively. (These estimaties include the factor 0.7 to account statistically for the beam squint's nonalignment with the velocity gradient.) These instrumental errors are fairly small compared to the most published field strengths, and we conclude that most measurements of Zeeman splitting in emission made with the HCRO telescope are reliable.

We emphasize that the instrumental errors discussed herein are under no circumstances characterized as fractional errors in $B_\parallel$. Rather, they depend on the local first and second derivatives of the 21 cm line velocity. Thus, our statement about reliability does not apply in the Galactic plane or for positions having unusually large velocity gradients.

This technique can be applied for any case in which the telescope sidelobes rotate more than 180° with respect to the sky. With an alt-az telescope, such rotation occurs naturally as many positions are tracked over the maximum range in our hour angle.

It is a real pleasure to dedicate this paper to my colleagues Alan Masters and Tom Troland. During the early development of the capability for these measurements at Hat Creek, Tom was a graduate student and we spent untold weeks at Hat Creek as pleasurable compatriots in an often frustrating undertaking. With Alan's cheerful cooperation in our many modifications to the telescope there was a symbiosis that carried the project forward, often in the face of discouragement and apparent disaster. Later, Alan—as the local telescope mechanic at Hat Creek—almost single-handedly bent the 85 foot telescope to his will and forced it to function, whether it wanted to or not. And he was the one who cut away the structure to make it possible to point toward the NCP.

I thank Alyssa Goodman for comments during the preparation of this paper. Most especially, I thank Dap Hartmann for providing me a copy of the Dwingeloo survey in advance of publication and, in addition, for his patient guidance in providing a detailed tutorial on how to use it. I acknowledge the unusually helpful comments of the referee, which stimuated me to expand the scope of this paper significantly. This work was supported in part by NSF grants to C. H. and to the Hat Creek Radio Observatory.

REFERENCES

Chu, T. S., & Turrin, R. H. 1973, IEEE Trans., AP-21, 339
Hartmann, D. 1994, Ph.D. thesis, University of Leiden
Hartmann, D., & Burton, W. B. 1996, Atlas of Galactic H I Emission (Cambridge: Cambridge Univ. Press), under contract
Heiles, C. 1988, ApJ, 324, 321
———. 1989, ApJ, 336, 808
———. 1990, in IAU Symp. 140, Galactic and Intergalactic Magnetic Fields, ed. R. Beck et al. (Dordrecht: Kluwer), 35
———. 1996, in Molecular Spectroscopy in the 1 to 10 GHz Range with the Upgraded Arecibo Telescope, ed. L. Olmi (Astrophys. Lett. Commun., in press)
Heiles, C., & Habing, H. J. 1974, A&AS, 14, 1
Heithausen, A., & Thaddeus, P. 1990, ApJ, 353, L49
Kaplan, W. 1952, Advanced Calculus (Reading: Addison-Wesley), 143
Kraus, J. D. 1966, Radio Astronomy (New York: McGraw-Hill), 108
Troland, T. H., & Heiles, C. 1982, ApJ, 252, 179 (TH)
Verschuur, G. L. 1969, ApJ, 156, 861
———. 1989, ApJ, 339, 163
———. 1993, BAAS, 25, 1466
———. 1995a, ApJ, 451, 624
———. 1995b, ApJ, 451, 645